How to cite: *Angew. Chem. Int. Ed.* **2023**, *62*, e202303910
doi.org/10.1002/anie.202303910

Computational Chemistry | Hot Paper

Origin of the Hydrophobic Behaviour of Hydrophilic CeO_2

Lorenzo Agosta, Daniel Arismendi-Arrieta, Mikhail Dzugutov, and Kersti Hermansson**

Abstract: The nature of the hydrophobicity found in rare-earth oxides is intriguing. The CeO_2 (100) surface, despite its strongly hydrophilic nature, exhibits hydrophobic behaviour when immersed in water. In order to understand this puzzling and counter-intuitive effect we performed a detailed analysis of the confined water structure and dynamics. We report here an ab-initio molecular dynamics simulation (AIMD) study which demonstrates that the first adsorbed water layer, in immediate contact with the hydroxylated CeO_2 surface, generates a hydrophobic interface with respect to the rest of the liquid water. The hydrophobicity is manifested in several ways: a considerable diffusion enhancement of the confined liquid water as compared with bulk water at the same thermodynamic condition, a weak adhesion energy and few H-bonds above the hydrophobic water layer, which may also sustain a water droplet. These findings introduce a new concept in water/rare-earth oxide interfaces: hydrophobicity mediated by specific water patterns on a hydrophilic surface.

Rare-earth oxides hold a special place among the metal oxides as they have been found experimentally to exhibit particularly high degrees of hydrophobicity.[1] Normally, metal oxide surfaces are hydrophilic due to the exposed under-coordinated metal and oxygen atoms, which create local dipoles where water molecules adsorb strongly.[2,3] The origin of the apparently intrinsic and unexpected hydrophobic behaviour of rare-earth oxides is unclear and many different and contradicting scenarios have been proposed in the literature. Azimi et al.[1] proposed that the inaccessibility of the 4f electrons of the metal ions for interacting with the adsorbing water oxygen could explain an intrinsic hydrophobicity. Carchini et al.[4] instead proposed that the mismatch between the rare-earths lattice oxygens and the adsorbed water network would overrule a natural hydrophilic character of these metal oxide surfaces making them hydrophobic. They also proposed that a change in the protonation state (induced by oxygen vacancies, surface reduction and/or the degree of water splitting) of a rare-earth oxide surface could switch its hydrophobic character to becoming a completely wet surface, in accordance with previous studies[5] that also discussed the role of surface hydroxylation.

Among the rare-earth oxides, ceria (CeO_2) has been seen as a reference material for the study of wetting properties due to its catalytic power for water splitting[6] and its high degree of apparent hydrophobicity, with water contact angles between 90° and 120°[1,7,8] (note: a large water contact angle is *the* definition of a hydrophobic surface). On the other hand, experimental investigations have shown that pristine ceria surfaces, even when stoichiometric, are actually hydrophilic but become hydrophobic after exposure to ambient conditions, more specifically by adsorbing hydrocarbon pollutants present in the environment.[9–12] The latter experimental results originate from X-Ray Photoelectron Spectroscopy (XPS) analysis of the ceria surfaces upon removal of water excess in order to measure the presence of adsorbed carbon species. Furthermore, the same studies reported a rapid increase of the water contact angle immediately after exposure of the ceria surface to the atmospheric moisture. Hence, a direct in situ measurement of the hydrophilic-hydrophobic transition at operando conditions *during* water exposure is missing, which makes it difficult to decipher the microscopic-level reasons behind this phenomenon.

All in all, it is fair to conclude that the current understanding of, and information about, the hydrophobicity / hydrophilicity of ceria is ambiguous. One can further note that the degree of CeO_2 hydrophobicity may depend on the specific crystal facets exposed (and their degree of hydroxylation) as suggested by density functional theory (DFT) based theoretical estimates of contact angles by Fronzi et al.;[13] in fact only the (100) facet was so far experimentally demonstrated to behave hydrophobically.[14,15]

In this Communication we report a first-principles Molecular Dynamics (AIMD) simulation addressing the origin of hydrophobicity of a hydrophilic CeO_2 surface. We demonstrate that the investigated (100) facet of CeO_2, although intrinsically hydrophilic, exhibits an effective hydrophobicity which is induced by the first adsorbed water layer rather than by the ceria surface itself. This water-induced hydrophobicity is tested in an AIMD droplet-on-a-fixed-layer simulation, which is found to retain a sustainable non-wetting character. Finally the molecular diffusion rate of water confined between the CeO_2 surfaces is found to be enhanced with respect to that in the bulk water at the same thermodynamic condition. Such a behaviour seemingly represents an anomaly for hydrophilic surfaces but it has

[*] Dr. L. Agosta, Dr. D. Arismendi-Arrieta, Prof. M. Dzugutov, Prof. K. Hermansson
Department of Chemistry-Ångström, Uppsala University, 751 21 Uppsala (Sweden)
E-mail: lorenzo.agosta@kemi.uu.se
kersti@kemi.uu.se

been observed for a number of hydrophobic materials and may be regarded as a signature of hydrophobicity.[16–21]

Theoretical studies of the clean CeO_2 (111) surface[4] and later also of clean (110) and (100) surfaces[13] have reported these to be hydrophobic. This conclusion was derived by estimating the water contact angle from expressions involving the interaction energy of a double ice layer with the CeO_2 surfaces. Such a computational procedure does not consider the contribution of liquid bulk water and disregards the water interaction beyond the double ice layer. Fully hydrated CeO_2 facets have indeed been investigated by computations, for example in the AIMD simulations by Camellone et al.[22] and by Ren et al.;[23] however hydrophobicity was not addressed in these studies. Our AIMD simulation considers a hydroxylated neutral CeO_2 (100) slab which consists of alternating Ce and O layers along the slab normal and a $c(2\times2)$ surface cell, resulting in an in-plane periodic simulation box of 10.86×10.86 Å^2 and a CeO_2 slab thickness of 10.6 Å. To prevent the slab from being polar, half of the oxygen atoms in the top layer were placed in the bottom layer, forming a 1/2 O-Ce-O-Ce-O-Ce-O-Ce-1/2 O sequence. The hydroxylated CeO_2 (100) surface was created by reconstructing the natural coordination of Ce atoms by adding 16 split water molecules (8 on each side of the CeO_2 (100) slab) resulting in 16 OH groups per slab side (see Figure 1). This structure was suggested by Kropp et al.[24] and it was later confirmed experimentally by a Nuclear Magnetic Resonance (NMR) study showing that the (100) surface is dominated by the existence of two OH populations with different chemical environments, one weakly interacting and one strongly interacting.[15] In our study, the vacuum region above the surface (about 37 Å thick) was filled with H_2O molecules corresponding to the water density at 1 atm and 310 K (see methods for further details).

The first important result is the formation of an almost rigid, well structured, flat layer on top of the hydroxylated CeO_2 (100) surface. This water layer is visible in Figure 1 (upper panel) as the peak labeled L_1 in the water oxygen density profile at 4 Å and by the representative snapshot displayed (Figure 1 lower panel and Figure 2a). The L_1 layer interacts with the surface hydroxyl groups (which we label L_0). After room-temperature MD relaxation, in the absence of the water slab above them, the hydroxide ions in L_0 exhibit two conformations, orthogonal and parallel to the surface ($OH_\perp$ and $OH_\parallel$). These OH configurations are maintained in the presence of liquid water and can be identified by the hydrogen density peaks at 1.5 and 2.4 Å in Figure 1. Our resulting MD structure, which features an L_0 layer interacting strongly with a water layer (L_1) above it, is

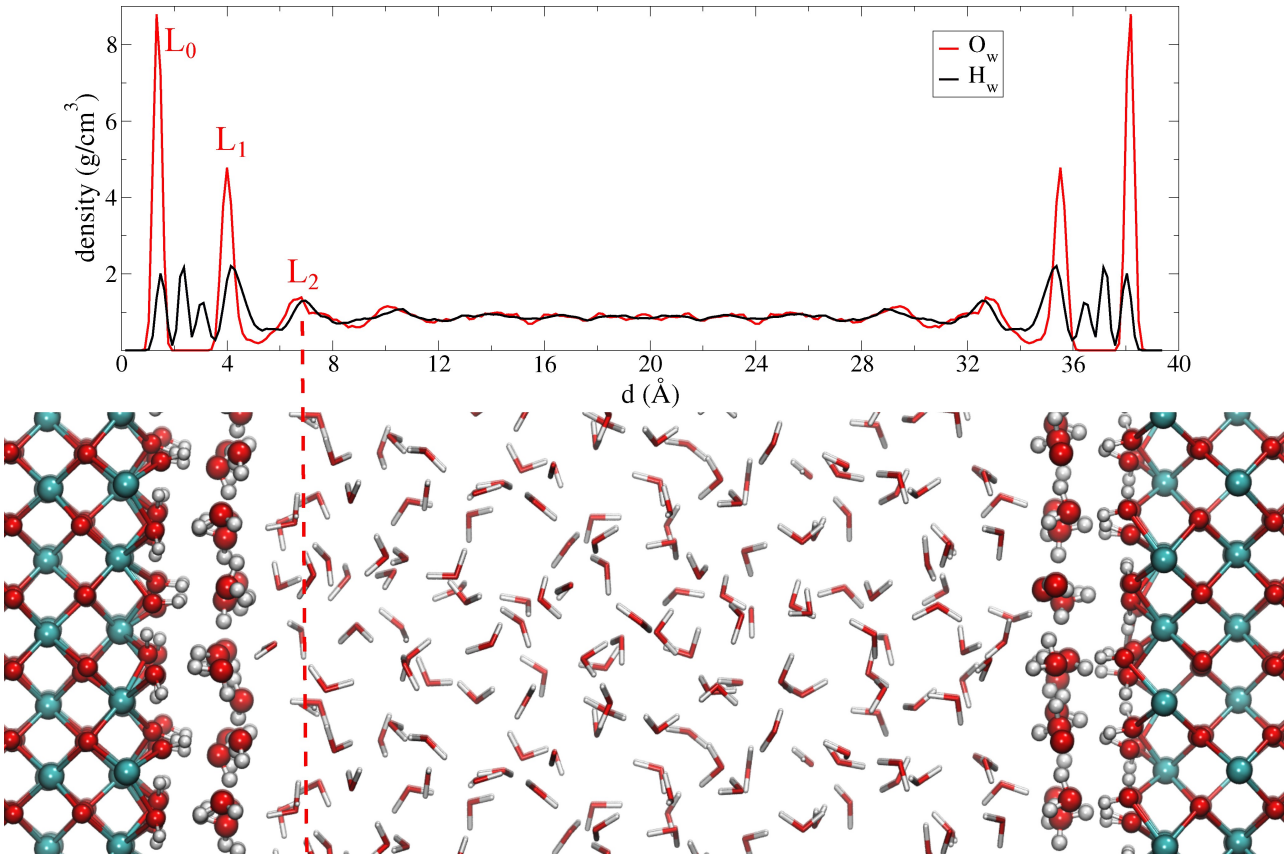

Figure 1. Contents of our periodic AIMD simulation box for a hydroxylated CeO_2 (100) surface in liquid water. The water oxygen and hydrogen density profiles (along the direction perpendicular to the surface) averaged along the MD trajectory are shown above the box. The CeO_2 (100) surface is stabilized by hydroxyl groups (layer L_0) which arrange themselves alternatively parallel and perpendicular to the ceria surface and form an intricate key-lock pattern with the first water layer (L_1).

consistent with the structures obtained by Kropp et al.[24] in their static DFT structure optimizations.

Also in our MD simulations, L_1 displays quite a rigid structure which is maintained along the full MD trajectory (see Figure S1 in Supporting Information), suggesting significant adhesion to L_0. This is also confirmed by a few separate single-point calculations from the AIMD trajectory where one single isolated water molecule from L_1 was left to interact with L_0 (all other water molecules were removed). This was done for two typical structures: the L_1 water donating a hydrogen bond to an $OH_{\parallel}$ in L_0, or the L_1 water accepting a hydrogen bond from $OH_{\perp}$ in L_0. The former has an interaction energy of 0.5 eV and the latter of 0.3 eV.

We furthermore computed the interaction energy (adhesion energy) between the layers L_1 and L_0 (see Table 1 and Supp. Info.), expressed per L_1 water molecule. The resulting energy is 0.53 eV per water molecule in L_1. This value is larger than our interaction energy per water molecule in bulk water, 0.45 eV (see Table 1). The extra energy contribution is due to the strong interaction with the hydroxylated CeO_2 (100) surface, confirming its hydrophilic nature. In the same way we computed the adhesion energy between L_1 and L_2, which instead resulted in 0.28 eV per water molecule, considerably lower that the respective value in bulk water. This implies a loss of energy for a water molecule in L_2 interacting with L_1 (which instead prefers the liquid water surroundings), which suggests an hydrophobic behaviour.

Returning now to the structure, inspection of the second water layer (L_2, peak maxima at 6.8 Å in the density profile) is also informative. We note in particular the low H density between the first and second layers (i.e. between L_1 and L_2). The hydrogen atoms belonging to L_1 water molecules lie almost entirely within this layer, or they point towards the CeO_2 surface (peak at 3.1 Å). Just a minority of the H atoms are oriented towards L_2. At the same time, the H atoms of the L_2 water molecules either lie completely in L_2 or they are, on average, slightly pointing away from L_1. This suggests only weak interaction between the L_1 and L_2 layers.[25]

Together, L_0 and L_1 form a bi-layer with a distorted square lattice. A top view snapshot of L_1 is presented in Figure 2a. Classical MD studies[26–28] have demonstrated that

Table 1: Adhesion energies involving the L_1 water layer, expressed in energy per L_1 water molecule, and compared with the average interaction energy in bulk water. (1st row:) The label "L_1-L_0" stands for the adhesion energy between L_1 and the "L_0+ceria" slab. (2nd row:) The label "L_1-L_2" here stands for the adhesion energy between it L_1 and the water film "above" it. (3rd row:) The intermolecular interaction energy per water molecule from a separate BLYP-D3 bulk simulation. The "L_1-L_2" interaction is seen to be considerably weaker than the other two cases. See Supp. Info. for the mathematical expressions used for the calculations.

Interaction type	Energy [eV]
L_0-L_1	0.53
L_1-L_2	0.28
bulk water	0.45

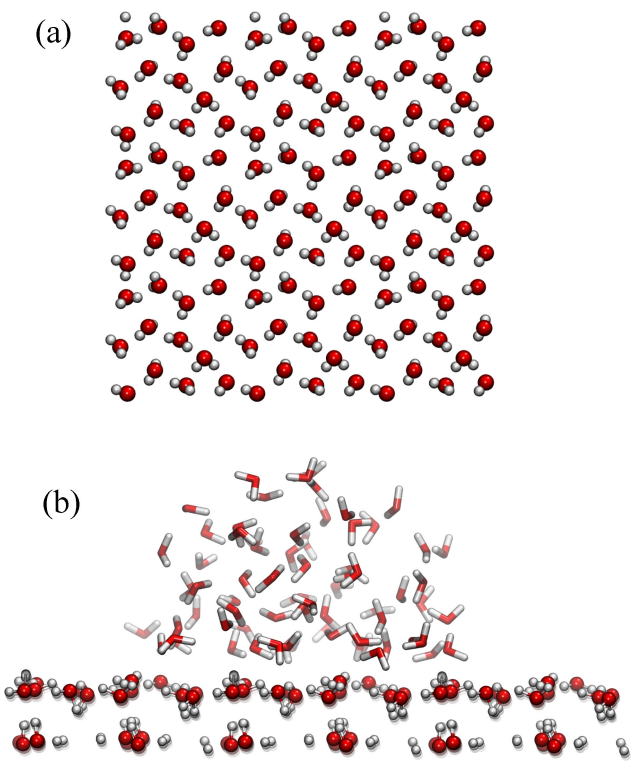

Figure 2. a) A snapshot from the AIMD simulation of the system in Figure 1, but here only the L_1 water layer is displayed. For visualization purposes it has been expanded periodically 3×3 times in the xy plane. b) Simulation of a water droplet (at 310 K) on a fixed L_1 structured water layer formed on the hydroxylated CeO_2 (100) surface. The droplet persists with a contact angle of circa 90° after 40 ps.

distorted and ordered FCC and hexagonal patterns of water molecules might exhibit hydrophobic character. Interesting cases are the bi-layer hexagonal ice (BHI) structure observed experimentally for water on graphene at low temperature,[29] water within hydrophobic nanopores,[30] water on clay mineral surfaces[31] and water on gold surfaces[32–34] at low temperature. The BHI pattern has been hypothesized to behave like a hydrophobic surface due to the locking pattern of hydrogen bonds which impedes the interaction with the surrounding water molecules. This was recently confirmed experimentally for polytetrafluoroethylene surfaces where the first hexagonal adsorbed water layer was shown to behave hydrophobically.[35] The square lattice of the water bi-layer that we observe in our simulation resemble the hydrogen-bond-locking pattern observed in the BHI structure.

As we mentioned, the existence of an ordered single water monolayer above the hydroxylated (100) ceria surface was predicted theoretically for a low water coverage scenario.[24] Here we confirm that such a structure (the L_1 layer) is stable also at room temperature and we furthermore explore the nature of its interactions with excess water added above it, which has not been discussed in the literature before. We propose that the locking mechanism and the interface structures may have significant consequences for the understanding of ceria hydrophobicity. This

might be the case also for the (111) facet of ceria, for which the formation of an ordered water layer was also predicted.[24]

To corroborate our hypothesis regarding the hydrophobicity of L_1, we performed an ab-initio MD simulation of a water droplet placed on the surface of an extended L_1 water layer (see methods). Figure 2b shows a characteristic simulation snapshot of the droplet interacting with the layer after 40 ps. It is clearly seen that the water droplet is not wetting the underlying water layer but forms a half-spherical shape typical of water droplets on hydrophobic surfaces. Although the simulation time might result too short for the characteristic relaxation time of the droplet interface, we note that in a simulation with the same droplet placed instead on the *bare* hydroxylated CeO_2 (100) surface, it completely spreads on the available surface after a few picoseconds. This supports the notion of the hydrophobic behaviour of L_1 compared to that of the bare hydroxylated CeO_2 (100) surface, in agreement with the interaction energy differences reported in Table 1. Similar computational experiments were performed using classical MD simulations for water droplets on TiO_2,[36] on Al_2O_3[37] and on regular water patterns,[26] providing support for the notion that certain structures of water in the first adsorbed water layer can increase the water contact angle.

In the following section we present results for water dynamics above the layer L_1 in our system, which provide compelling evidence in support of our conjecture that the structure of the first adsorbed water layer plays a key role for the hydrophobicity of ceria (100).

The effects of the proximity of a confining wall on liquid dynamics have been explored in a number of studies.[16,39,40] It was found that a wide range of liquids demonstrate enhanced dynamics close to non-interactive walls. In the case of water, the results demonstrate a sharp difference between the effects of hydrophilic and hydrophobic confining surfaces: while the former suppresses water dynamics[16,38–41] the latter enhances them.[16–21] This is the case for water in proximity of hydrophilic TiO_2 surface which was found to drastically slow down both translational and rotational water diffusion.[42–45] On the other hand, a strong enhancement of translational diffusion was observed in a similar simulation of water confined between two flat walls of graphene,[18] which is well-known to exhibit a pronounced hydrophobicity. Thus, the comparison of the diffusion rate in water close to confining surfaces with that in the bulk water can be regarded as a robust test of the surface hydrophobicity.

Following these arguments, we investigated both the translational and rotational diffusion of the water in our CeO_2 model system in order to find supporting evidence for our conjecture that the water bilayer previously described behaves as a hydrophobic surface with respect to the rest of the water. Our first important observation is a significant enhancement of the translational diffusion in the water confined between the CeO_2 (100) surfaces. Figure 3a shows the three-dimensional (3D) Mean Square Displacement (MSD) of water molecules confined between CeO_2 (100) and TiO_2 anatase (101) surfaces as compared with the MSD

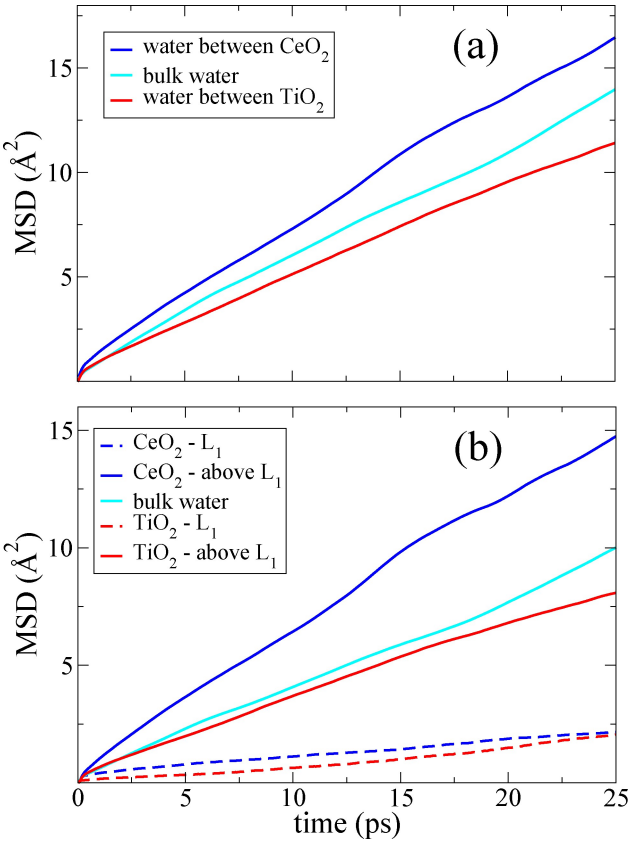

Figure 3. MSD of water confined between CeO_2 (100) surfaces and between TiO_2 anatase (101) surfaces, respectively, compared with bulk water at the same temperature and density. a) The total 3D MSD, and b) the lateral 2D MSD. The overall 3D diffusion enhancement is mainly attributed to the lateral component. The water data on the TiO_2 anatase (101) surface are taken from Ref.[38]

calculated for the bulk water at the same thermodynamic conditions. It is evident that the confinement between the supposedly hydrophilic CeO_2 (100) surfaces enhances the water diffusion, while the opposite behaviour is observed for the TiO_2 case.

We also calculated the 2D MSD for L_1 and the water above L_1. The results are presented in Figure 3b, where the lateral MSD parallel to the CeO_2 and TiO_2 surfaces are compared with the 2D MSD of bulk water at the same temperature and water density. Here we note that practically no diffusion is observed in L_1 for neither CeO_2 nor TiO_2, confirming their rigid structures. The water above L_1 for CeO_2 instead displays significant lateral diffusion enhancement relative to the bulk water and the TiO_2 surface. This observation indicates that the average interaction between L_1 and L_2 on CeO_2 is weaker than water between the hydrophilic TiO_2 surface, almost as weak as the case of water on a non-interacting confining surface.[17–19] A similar effect was also reported for a water layer next to a repulsive model surface[20] and for a water layer on hydrophobic Lennard-Jones surfaces.[21]

We note that Cicero et al.,[18] using ab-initio MD simulations, demonstrated that the dipole-dipole correlation

in water confined between hydrophobic graphene sheets decayed at the same rate as that of bulk water, when the graphene surface separation is 25 Å. In our simulation the dipole correlation function calculated for water between L_1 layers on CeO_2 separated by 28 Å (between z = 6 Å and z = 34 Å in Fig. Figure 1) closely agrees with the dipole correlation of bulk water, supporting the hydrophobic effect of L_1 (see Figure S2 in Supp. Info.).

These results show that translational and rotational dynamics of water confined between the CeO_2 (100) surfaces match the behaviour of water confined between hydrophobic graphene surfaces. On the other hand, the observed dynamics is quite different from that in the water confined between TiO_2 surfaces. We regard this observation as a strong evidence of the hydrophobic nature of the L_1 layer.

The main result of this work is our deciphering of the hydrophobic origin of the hydrophilic hydroxylated ceria (100) facet. A first-principles AIMD simulation of liquid water "on top of" this facet was performed and the following key observations and conclusions were made. *(1)* An ordered water layer was found to form on the hydroxylated surface, the two together ($L_0 + L_1$) forming an H-bonded key-lock pattern which persists at room temperature. *(2)* The ordered water layer (L_1) interacts only weakly with the water film above it (L_2), as evidenced both by the scarcity of H-bonds between the layer and the film above and by the modest interaction energy between them. *(3)* The ordered water layer formed on the ceria (100) facet thus makes it hydrophobic. This observation is consistent with the results of a separate AIMD simulation for a water droplet deposited on the ordered water layer. *(4)* The hydrophobicity of such an ordered layer manifests itself in the enhancement of water diffusion as compared to bulk water. This diffusion enhancement has been earlier observed in water confined between fully hydrophobic surfaces.[16–21]

Altogether our results reveal an atomistic mechanism which explains the origin of the natural hydrophobicity of the hydrophilic ceria (100) and possibly of other rare-earth oxides as well: hydrophobicity triggered by specific water patterns on hydrophilic surfaces.

Acknowledgements

We acknowledge the Swedish Research Council (Vetenskapsrådet, project number 2021-06757) and the National Strategic e-Science program eSSENCE for funding. We also acknowledge the Swedish National Infrastructure for Computing (SNIC/NAISS) for providing the computer resources used in this project.

Conflict of Interest

The authors declare no conflicts of interest.

Data Availability Statement

The data that support the findings of this study are available from the corresponding authors upon reasonable request.

Keywords: Hydrophobicity · Cerium Oxide · Water · Ab-initio Molecular Dynamics · Interfaces

[1] G. Azimi, R. Dhiman, H.-M. Kwon, A. T. Paxson, K. K. Varanasi, *Nat. Mater.* **2013**, *12*, 315.
[2] R. Mu, Z. Zhao, Z. Dohnálek, J. Gong, *Chem. Rev.* **2017**, *117*, 1785.
[3] M. J. Limo, A. Sola-Rabada, E. Boix, V. Thota, Z. C. Westcott, V. Puddu, C. C. Perry, *Chem. Rev.* **2018**, *118*, 11118.
[4] G. Carchini, M. García-Melchor, Z. Łodziana, N. López, *ACS Appl. Mater. Interfaces* **2016**, *8*, 152.
[5] S. Khan, G. Azimi, B. Yildiz, K. K. Varanasi, *Appl. Phys. Lett.* **2015**, *106*, 061601.
[6] T. Montini, M. Melchionna, M. Monai, P. Fornasiero, *Chem. Rev.* **2016**, *116*, 5987.
[7] X. Zheng, L. Liu, X. Zhou, *Colloid J.* **2014**, *76*, 558–563.
[8] M. S. Kabir, P. Munroe, V. Gonçales, Z. Zhou, Z. Xie, *Surf. Coat. Technol.* **2018**, *349*, 667.
[9] D. J. Preston, N. Miljkovic, J. Sack, R. Enright, J. Queeney, E. N. Wang, *Appl. Phys. Lett.* **2014**, *105*, 011601.
[10] R. Lundy, C. Byrne, J. Bogan, K. Nolan, M. N. Collins, E. Dalton, R. Enright, *ACS Appl. Mater. Interfaces* **2017**, *9*, 13751.
[11] E. Kulah, L. Marot, R. Steiner, A. Romanyuk, T. Jung, A. Wackerlin, E. Meyer, *Sci. Rep.* **2017**, *7*, 43369.
[12] J. Bae, I. A. Samek, P. C. Stair, R. Q. Snurr, *Langmuir* **2019**, *35*, 5762.
[13] M. Fronzi, M. H. N. Assadi, D. A. Hanaor, *Appl. Phys. Lett.* **2019**, *478*, 68.
[14] G. S. Herman, Y. J. Kim, S. A. Chambers, C. H. F. Peden, *Langmuir* **1999**, *15*, 3993.
[15] L. Gill, A. Beste, B. Chen, M. Li, A. K. P. Mann, S. H. Overbury, E. W. Hagaman, *J. Phys. Chem. C* **2017**, *121*, 7450.
[16] I. N. Tsimpanogiannis, O. A. Moultos, L. F. M. Franco, M. B. de M Spera, M. Erdős, I. G. Economou, *Mol. Simul.* **2019**, *45*, 425.
[17] A. Kayal, A. Chandra, *J. Chem. Phys.* **2017**, *147*, 164704.
[18] G. Cicero, J. C. Grossman, E. Schwegler, F. Gygi, G. Galli, *J. Am. Chem. Soc.* **2008**, *130*, 1871, pMID: 18211065.
[19] M. Chiricotto, F. Martelli, G. Giunta, P. Carbone, *J. Phys. Chem. C* **2021**, *125*, 6367.
[20] P. Kumar, S. V. Buldyrev, F. W. Starr, N. Giovambattista, H. E. Stanley, *Phys. Rev. E* **2005**, *72*, 051503.
[21] S. H. Lee, P. J. Rossky, *J. Chem. Phys.* **1994**, *100*, 3334.
[22] M. Farnesi Camellone, F. Negreiros Ribeiro, L. Szabová, Y. Tateyama, S. Fabris, *J. Am. Chem. Soc.* **2016**, *138*, 11560.
[23] Z. Ren, N. Liu, B. Chen, J. Li, D. Mei, *J. Phys. Chem. C* **2018**, *122*, 4828.
[24] T. Kropp, J. Paier, J. Sauer, *J. Phys. Chem. C* **2017**, *121*, 21571.
[25] S. Pezzotti, A. Serva, F. Sebastiani, F. Brigano, D. Galimberti, L. Potier, S. Alfarano, G. Schwaab, M. Havenith, M. Gaigeot, *J. Phys. Chem. Lett.* **2021**, *12*, 3827–3836.
[26] C. Qi, X. Lei, B. Zhou, C. Wang, Y. Zheng, *J. Chem. Phys.* **2019**, *150*, 234703.
[27] C. Wang, C. Qi, Y. Tu, X. Nie, S. Liang, *Phys. Rev. Mater.* **2019**, *3*, 065602.
[28] D. T. Limmer, A. P. Willard, P. Madden, D. Chandler, *Proc. Natl. Acad. Sci. USA* **2013**, *110*, 4200.
[29] G. A. Kimmel, J. Matthiesen, M. Baer, C. J. Mundy, N. G. Petrik, R. S. Smith, Z. Dohnálek, B. D. Kay, *J. Am. Chem. Soc.* **2009**, *131*, 12838.

[30] K. Koga, X. C. Zeng, H. Tanaka, *Phys. Rev. Lett.* **1997**, *79*, 5262.
[31] X. L. Hu, A. Michaelides, *Surf. Sci.* **2008**, *602*, 960.
[32] D. Stacchiola, J. B. Park, P. Liu, S. Ma, F. Yang, D. E. Starr, E. Muller, P. Sutter, J. Hrbek, *J. Phys. Chem. C* **2009**, *113*, 15102.
[33] R. Ma, D. Cao, C. Zhu, Y. Tian, J. Peng, J. Guo, J. Chen, X.-Z. Li, J. S. F. Francisco, X. C. Zeng, L.-M. X. Xu, E.-G. W. Wang, Y. Jiang, *Nature* **2020**, *577*, 60.
[34] P. Yang, C. Zhang, W. Sun, J. Dong, D. Cao, J. Guo, Y. Jiang, *Phys. Rev. Lett.* **2022**, *129*, 046001.
[35] J. Zhang, J. Tan, R. Pei, S. Ye, Y. Luo, *J. Am. Chem. Soc.* **2021**, *143*, 13074.
[36] M. Qu, G. Huang, X. Liu, X. Nie, C. Qi, H. Wang, J. Hu, H. Fang, Y. Gao, W.-T. Liu, J. S. Francisco, C. Wang, *Chem. Sci.* **2022**, *13*, 10546.
[37] A. Phan, T. A. Ho, D. R. Cole, A. Striolo, *J. Phys. Chem. C* **2012**, *116*, 15962.
[38] L. Agosta, E. G. Brandt, A. P. Lyubartsev, *J. Chem. Phys.* **2017**, *147*, 024704.
[39] S. Romero-Vargas Castrillón, N. Giovambattista, I. A. Aksay, P. G. Debenedetti, *J. Phys. Chem. B* **2009**, *113*, 1438.
[40] S. Romero-Vargas Castrillón, N. Giovambattista, I. A. Aksay, P. G. Debenedetti, *J. Phys. Chem. B* **2009**, *113*, 7973.
[41] S. Cerveny, F. Mallamace, J. Swenson, M. Vogel, L. Xu, *Chem. Rev.* **2016**, *116*, 7608.
[42] L. Agosta, M. Dzugutov, K. Hermansson, *J. Chem. Phys.* **2021**, *154*, 094708.
[43] E. Mamontov, L. Vlcek, D. J. Wesolowski, P. T. Cummings, W. Wang, L. M. Anovitz, J. Rosenqvist, C. M. Brown, V. Garcia Sakai, *J. Phys. Chem. C* **2007**, *111*, 4328.
[44] M. Předota, A. V. Bandura, P. T. Cummings, J. D. Kubicki, D. J. Wesolowski, A. A. Chialvo, M. L. Machesky, *J. Phys. Chem. B* **2004**, *108*, 12049.
[45] R. S. Kavathekar, N. J. English, J. MacElroy, *Mol. Phys.* **2011**, *109*, 2645.

Manuscript received: March 17, 2023
Accepted manuscript online: April 3, 2023
Version of record online: June 20, 2023